

An inclusive search for the Higgs boson in the four-lepton final state at CDF

T. Aaltonen,²¹ B. Álvarez González^{z,9} S. Amerio,⁴⁰ D. Amidei,³² A. Anastassov^{x,15} A. Annovi,¹⁷ J. Antos,¹² G. Apollinari,¹⁵ J.A. Appel,¹⁵ T. Arisawa,⁵⁴ A. Artikov,¹³ J. Asaadi,⁴⁹ W. Ashmanskas,¹⁵ B. Auerbach,⁵⁷ A. Aurisano,⁴⁹ F. Azfar,³⁹ W. Badgett,¹⁵ T. Bae,²⁵ A. Barbaro-Galtieri,²⁶ V.E. Barnes,⁴⁴ B.A. Barnett,²³ P. Barria^{hh,42} P. Bartos,¹² M. Bauc^{ff,40} F. Bedeschi,⁴² S. Behari,²³ G. Bellettini^{gg,42} J. Bellinger,⁵⁶ D. Benjamin,¹⁴ A. Beretvas,¹⁵ A. Bhatti,⁴⁶ D. Bisello^{ff,40} I. Bizjak,²⁸ K.R. Bland,⁵ B. Blumenfeld,²³ A. Bocci,¹⁴ A. Bodek,⁴⁵ D. Bortoletto,⁴⁴ J. Boudreau,⁴³ A. Boveia,¹¹ L. Brigliadori^{ee,6} C. Bromberg,³³ E. Brucken,²¹ J. Budagov,¹³ H.S. Budd,⁴⁵ K. Burkett,¹⁵ G. Busetto^{ff,40} P. Bussey,¹⁹ A. Buzatu,³¹ A. Calamba,¹⁰ C. Calancha,²⁹ S. Camarda,⁴ M. Campanelli,²⁸ M. Campbell,³² F. Canelli^{11,15} B. Carls,²² D. Carlsmith,⁵⁶ R. Carosi,⁴² S. Carrillo^{m,16} S. Carron,¹⁵ B. Casal^{k,9} M. Casarsa,⁵⁰ A. Castro^{ee,6} P. Catastini,²⁰ D. Cauz,⁵⁰ V. Cavaliere,²² M. Cavalli-Sforza,⁴ A. Cerri^{f,26} L. Cerrito^{s,28} Y.C. Chen,¹ M. Chertok,⁷ G. Chiarelli,⁴² G. Chlachidze,¹⁵ F. Chlebana,¹⁵ K. Cho,²⁵ D. Chokheli,¹³ W.H. Chung,⁵⁶ Y.S. Chung,⁴⁵ M.A. Ciocci^{hh,42} A. Clark,¹⁸ C. Clarke,⁵⁵ G. Compostella^{ff,40} M.E. Convery,¹⁵ J. Conway,⁷ M. Corbo,¹⁵ M. Cordelli,¹⁷ C.A. Cox,⁷ D.J. Cox,⁷ F. Crescioli^{gg,42} J. Cuevas^{z,9} R. Culbertson,¹⁵ D. Dagenhart,¹⁵ N. d'Ascenzo^{w,15} M. Datta,¹⁵ P. de Barbaro,⁴⁵ M. Dell'Orso^{gg,42} L. Demortier,⁴⁶ M. Deninno,⁶ F. Devoto,²¹ M. d'Errico^{ff,40} A. Di Canto^{gg,42} B. Di Ruzza,¹⁵ J.R. Dittmann,⁵ M. D'Onofrio,²⁷ S. Donati^{gg,42} P. Dong,¹⁵ M. Dorigo,⁵⁰ T. Dorigo,⁴⁰ K. Ebina,⁵⁴ A. Elagin,⁴⁹ A. Eppig,³² R. Erbacher,⁷ S. Errede,²² N. Ershaidat^{dd,15} R. Eusebi,⁴⁹ S. Farrington,³⁹ M. Feindt,²⁴ J.P. Fernandez,²⁹ R. Field,¹⁶ G. Flanagan^{u,15} R. Forrest,⁷ M.J. Frank,⁵ M. Franklin,²⁰ J.C. Freeman,¹⁵ Y. Funakoshi,⁵⁴ I. Furic,¹⁶ M. Gallinaro,⁴⁶ J.E. Garcia,¹⁸ A.F. Garfinkel,⁴⁴ P. Garosi^{hh,42} H. Gerberich,²² E. Gerchtein,¹⁵ S. Giagu,⁴⁷ V. Giakoumopoulou,³ P. Giannetti,⁴² K. Gibson,⁴³ C.M. Ginsburg,¹⁵ N. Giokaris,³ P. Giromini,¹⁷ G. Giurgiu,²³ V. Glagolev,¹³ D. Glenzinski,¹⁵ M. Gold,³⁵ D. Goldin,⁴⁹ N. Goldschmidt,¹⁶ A. Golossanov,¹⁵ G. Gomez,⁹ G. Gomez-Ceballos,³⁰ M. Goncharov,³⁰ O. González,²⁹ I. Gorelov,³⁵ A.T. Goshaw,¹⁴ K. Goulianos,⁴⁶ S. Grinstein,⁴ C. Grosso-Pilcher,¹¹ R.C. Group^{53,15} J. Guimaraes da Costa,²⁰ S.R. Hahn,¹⁵ E. Halkiadakis,⁴⁸ A. Hamaguchi,³⁸ J.Y. Han,⁴⁵ F. Happacher,¹⁷ K. Hara,⁵¹ D. Hare,⁴⁸ M. Hare,⁵² R.F. Harr,⁵⁵ K. Hatakeyama,⁵ C. Hays,³⁹ M. Heck,²⁴ J. Heinrich,⁴¹ M. Herndon,⁵⁶ S. Hewamanage,⁵ A. Hocker,¹⁵ W. Hopkins^{g,15} D. Horn,²⁴ S. Hou,¹ R.E. Hughes,³⁶ M. Hurwitz,¹¹ U. Husemann,⁵⁷ N. Hussain,³¹ M. Hussein,³³ J. Huston,³³ G. Introzzi,⁴² M. Iori^{jj,47} A. Ivanov^{p,7} E. James,¹⁵ D. Jang,¹⁰ B. Jayatilaka,¹⁴ E.J. Jeon,²⁵ S. Jindariani,¹⁵ M. Jones,⁴⁴ K.K. Joo,²⁵ S.Y. Jun,¹⁰ T.R. Junk,¹⁵ T. Kamon^{25,49} P.E. Karchin,⁵⁵ A. Kashi,⁵ Y. Kato^{o,38} W. Ketchum,¹¹ J. Keung,⁴¹ V. Khotilovich,⁴⁹ B. Kilminster,¹⁵ D.H. Kim,²⁵ H.S. Kim,²⁵ J.E. Kim,²⁵ M.J. Kim,¹⁷ S.B. Kim,²⁵ S.H. Kim,⁵¹ Y.K. Kim,¹¹ Y.J. Kim,²⁵ N. Kimura,⁵⁴ M. Kirby,¹⁵ S. Klimentenko,¹⁶ K. Knoepfel,¹⁵ K. Kondo^{*,54} D.J. Kong,²⁵ J. Konigsberg,¹⁶ A.V. Kotwal,¹⁴ M. Kreps,²⁴ J. Kroll,⁴¹ D. Krop,¹¹ M. Kruse,¹⁴ V. Krutelyov^{c,49} T. Kuhr,²⁴ M. Kurata,⁵¹ S. Kwang,¹¹ A.T. Laasanen,⁴⁴ S. Lami,⁴² S. Lammel,¹⁵ M. Lancaster,²⁸ R.L. Lander,⁷ K. Lannon^{y,36} A. Lath,⁴⁸ G. Latino^{hh,42} T. LeCompte,² E. Lee,⁴⁹ H.S. Lee^{q,11} J.S. Lee,²⁵ S.W. Lee^{bb,49} S. Leo^{gg,42} S. Leone,⁴² J.D. Lewis,¹⁵ A. Limosani^{t,14} C.-J. Lin,²⁶ M. Lindgren,¹⁵ E. Lipeles,⁴¹ A. Lister,¹⁸ D.O. Litvintsev,¹⁵ C. Liu,⁴³ H. Liu,⁵³ Q. Liu,⁴⁴ T. Liu,¹⁵ S. Lockwitz,⁵⁷ A. Loginov,⁵⁷ D. Lucchesi^{ff,40} J. Lueck,²⁴ P. Lujan,²⁶ P. Lukens,¹⁵ G. Lungu,⁴⁶ J. Lys,²⁶ R. Lysak^{e,12} R. Madrak,¹⁵ K. Maeshima,¹⁵ P. Maestro^{hh,42} S. Malik,⁴⁶ G. Manca^{a,27} A. Manousakis-Katsikakis,³ F. Margaroli,⁴⁷ C. Marino,²⁴ M. Martínez,⁴ P. Mastrandrea,⁴⁷ K. Matera,²² M.E. Mattson,⁵⁵ A. Mazzacane,¹⁵ P. Mazzanti,⁶ K.S. McFarland,⁴⁵ P. McIntyre,⁴⁹ R. McNulty^{j,27} A. Mehta,²⁷ P. Mehtala,²¹ C. Mesropian,⁴⁶ T. Miao,¹⁵ D. Mietlicki,³² A. Mitra,¹ H. Miyake,⁵¹ S. Moed,¹⁵ N. Moggi,⁶ M.N. Mondragon^{m,15} C.S. Moon,²⁵ R. Moore,¹⁵ M.J. Morello^{ii,42} J. Morlock,²⁴ P. Movilla Fernandez,¹⁵ A. Mukherjee,¹⁵ Th. Muller,²⁴ P. Murat,¹⁵ M. Mussini^{ee,6} J. Nachtman^{n,15} Y. Nagai,⁵¹ J. Naganoma,⁵⁴ I. Nakano,³⁷ A. Napier,⁵² J. Nett,⁴⁹ C. Neu,⁵³ M.S. Neubauer,²² J. Nielsen^{d,26} L. Nodulman,² S.Y. Noh,²⁵ O. Norriella,²² L. Oakes,³⁹ S.H. Oh,¹⁴ Y.D. Oh,²⁵ I. Oksuzian,⁵³ T. Okusawa,³⁸ R. Orava,²¹ L. Ortolan,⁴ S. Pagan Griso^{ff,40} C. Pagliarone,⁵⁰ E. Palencia^{f,9} V. Papadimitriou,¹⁵ A.A. Paramonov,² J. Patrick,¹⁵ G. Pauletta^{kk,50} M. Paulini,¹⁰ C. Paus,³⁰ D.E. Pellett,⁷ A. Penzo,⁵⁰ T.J. Phillips,¹⁴ G. Piacentino,⁴² E. Pianori,⁴¹ J. Pilot,³⁶ K. Pitts,²² C. Plager,⁸ L. Pondrom,⁵⁶ S. Poprocki^{g,15} K. Potamianos,⁴⁴ F. Prokoshin^{cc,13} A. Pranko,²⁶ F. Ptohos^{h,17} G. Punzi^{gg,42} A. Rahaman,⁴³ V. Ramakrishnan,⁵⁶ N. Ranjan,⁴⁴ I. Redondo,²⁹ P. Renton,³⁹ M. Rescigno,⁴⁷ T. Riddick,²⁸ F. Rimondi^{ee,6} L. Ristori^{42,15} A. Robson,¹⁹ T. Rodrigo,⁹ T. Rodriguez,⁴¹ E. Rogers,²² S. Rolli^{i,52} R. Roser,¹⁵ F. Ruffini^{hh,42} A. Ruiz,⁹ J. Russ,¹⁰ V. Rusu,¹⁵ A. Safonov,⁴⁹ W.K. Sakumoto,⁴⁵ Y. Sakurai,⁵⁴ L. Santi^{kk,50} K. Sato,⁵¹ V. Savelyev^{w,15} A. Savoy-Navarro^{aa,15} P. Schlabach,¹⁵ A. Schmidt,²⁴ E.E. Schmidt,¹⁵ T. Schwarz,¹⁵ L. Scodellaro,⁹ A. Scribano^{hh,42} F. Scuri,⁴² S. Seidel,³⁵ Y. Seiya,³⁸ A. Semenov,¹³ F. Sforza^{hh,42} S.Z. Shalhout,⁷ T. Shears,²⁷

P.F. Shepard,⁴³ M. Shimojima^v,⁵¹ M. Shochet,¹¹ I. Shreyber-Tecker,³⁴ A. Simonenko,¹³ P. Sinervo,³¹ K. Sliwa,⁵² J.R. Smith,⁷ F.D. Snider,¹⁵ A. Soha,¹⁵ V. Sorin,⁴ H. Song,⁴³ P. Squillacioti^{hh},⁴² M. Stancari,¹⁵ R. St. Denis,¹⁹ B. Stelzer,³¹ O. Stelzer-Chilton,³¹ D. Stentz^x,¹⁵ J. Strologas,³⁵ G.L. Strycker,³² Y. Sudo,⁵¹ A. Sukhanov,¹⁵ I. Suslov,¹³ K. Takemasa,⁵¹ Y. Takeuchi,⁵¹ J. Tang,¹¹ M. Tecchio,³² P.K. Teng,¹ J. Thom^g,¹⁵ J. Thome,¹⁰ G.A. Thompson,²² E. Thomson,⁴¹ D. Toback,⁴⁹ S. Tokar,¹² K. Tollefson,³³ T. Tomura,⁵¹ D. Tonelli,¹⁵ S. Torre,¹⁷ D. Torretta,¹⁵ P. Totaro,⁴⁰ M. Trovatoⁱⁱ,⁴² F. Ukegawa,⁵¹ S. Uozumi,²⁵ A. Varganov,³² F. Vázquez^m,¹⁶ G. Velev,¹⁵ C. Vellidis,¹⁵ M. Vidal,⁴⁴ I. Vila,⁹ R. Vilar,⁹ J. Vizán,⁹ M. Vogel,³⁵ G. Volpi,¹⁷ P. Wagner,⁴¹ R.L. Wagner,¹⁵ T. Wakisaka,³⁸ R. Wallny,⁸ S.M. Wang,¹ A. Warburton,³¹ D. Waters,²⁸ W.C. Wester III,¹⁵ D. Whiteson^b,⁴¹ A.B. Wicklund,² E. Wicklund,¹⁵ S. Wilbur,¹¹ F. Wick,²⁴ H.H. Williams,⁴¹ J.S. Wilson,³⁶ P. Wilson,¹⁵ B.L. Winer,³⁶ P. Wittich^g,¹⁵ S. Wolbers,¹⁵ H. Wolfe,³⁶ T. Wright,³² X. Wu,¹⁸ Z. Wu,⁵ K. Yamamoto,³⁸ D. Yamato,³⁸ T. Yang,¹⁵ U.K. Yang^r,¹¹ Y.C. Yang,²⁵ W.-M. Yao,²⁶ G.P. Yeh,¹⁵ K. Yiⁿ,¹⁵ J. Yoh,¹⁵ K. Yorita,⁵⁴ T. Yoshida^l,³⁸ G.B. Yu,¹⁴ I. Yu,²⁵ S.S. Yu,¹⁵ J.C. Yun,¹⁵ A. Zanetti,⁵⁰ Y. Zeng,¹⁴ C. Zhou,¹⁴ and S. Zucchelli^{ee6}

(CDF Collaboration[†])

¹*Institute of Physics, Academia Sinica, Taipei, Taiwan 11529, Republic of China*

²*Argonne National Laboratory, Argonne, Illinois 60439, USA*

³*University of Athens, 157 71 Athens, Greece*

⁴*Institut de Física d'Altes Energies, ICREA, Universitat Autònoma de Barcelona, E-08193, Bellaterra (Barcelona), Spain*

⁵*Baylor University, Waco, Texas 76798, USA*

⁶*Istituto Nazionale di Fisica Nucleare Bologna, ^{ee}University of Bologna, I-40127 Bologna, Italy*

⁷*University of California, Davis, Davis, California 95616, USA*

⁸*University of California, Los Angeles, Los Angeles, California 90024, USA*

⁹*Instituto de Física de Cantabria, CSIC-University of Cantabria, 39005 Santander, Spain*

¹⁰*Carnegie Mellon University, Pittsburgh, Pennsylvania 15213, USA*

¹¹*Enrico Fermi Institute, University of Chicago, Chicago, Illinois 60637, USA*

¹²*Comenius University, 842 48 Bratislava, Slovakia; Institute of Experimental Physics, 040 01 Kosice, Slovakia*

¹³*Joint Institute for Nuclear Research, RU-141980 Dubna, Russia*

¹⁴*Duke University, Durham, North Carolina 27708, USA*

¹⁵*Fermi National Accelerator Laboratory, Batavia, Illinois 60510, USA*

¹⁶*University of Florida, Gainesville, Florida 32611, USA*

¹⁷*Laboratori Nazionali di Frascati, Istituto Nazionale di Fisica Nucleare, I-00044 Frascati, Italy*

¹⁸*University of Geneva, CH-1211 Geneva 4, Switzerland*

¹⁹*Glasgow University, Glasgow G12 8QQ, United Kingdom*

²⁰*Harvard University, Cambridge, Massachusetts 02138, USA*

²¹*Division of High Energy Physics, Department of Physics,*

University of Helsinki and Helsinki Institute of Physics, FIN-00014, Helsinki, Finland

²²*University of Illinois, Urbana, Illinois 61801, USA*

²³*The Johns Hopkins University, Baltimore, Maryland 21218, USA*

²⁴*Institut für Experimentelle Kernphysik, Karlsruhe Institute of Technology, D-76131 Karlsruhe, Germany*

²⁵*Center for High Energy Physics: Kyungpook National University,*

Daegu 702-701, Korea; Seoul National University, Seoul 151-742,

Korea; Sungkyunkwan University, Suwon 440-746,

Korea; Korea Institute of Science and Technology Information,

Daejeon 305-806, Korea; Chonnam National University, Gwangju 500-757,

Korea; Chonbuk National University, Jeonju 561-756, Korea

²⁶*Ernest Orlando Lawrence Berkeley National Laboratory, Berkeley, California 94720, USA*

²⁷*University of Liverpool, Liverpool L69 7ZE, United Kingdom*

²⁸*University College London, London WC1E 6BT, United Kingdom*

²⁹*Centro de Investigaciones Energeticas Medioambientales y Tecnológicas, E-28040 Madrid, Spain*

³⁰*Massachusetts Institute of Technology, Cambridge, Massachusetts 02139, USA*

³¹*Institute of Particle Physics: McGill University, Montréal, Québec,*

Canada H3A 2T8; Simon Fraser University, Burnaby, British Columbia,

Canada V5A 1S6; University of Toronto, Toronto, Ontario,

Canada M5S 1A7; and TRIUMF, Vancouver, British Columbia, Canada V6T 2A3

³²*University of Michigan, Ann Arbor, Michigan 48109, USA*

³³*Michigan State University, East Lansing, Michigan 48824, USA*

³⁴*Institution for Theoretical and Experimental Physics, ITEP, Moscow 117259, Russia*

³⁵*University of New Mexico, Albuquerque, New Mexico 87131, USA*

³⁶*The Ohio State University, Columbus, Ohio 43210, USA*

³⁷*Okayama University, Okayama 700-8530, Japan*

³⁸*Osaka City University, Osaka 588, Japan*

- ³⁹University of Oxford, Oxford OX1 3RH, United Kingdom
⁴⁰Istituto Nazionale di Fisica Nucleare, Sezione di Padova-Trento, ^{fj}University of Padova, I-35131 Padova, Italy
⁴¹University of Pennsylvania, Philadelphia, Pennsylvania 19104, USA
⁴²Istituto Nazionale di Fisica Nucleare Pisa, ^{gg}University of Pisa,
^{hh}University of Siena and ⁱⁱScuola Normale Superiore, I-56127 Pisa, Italy
⁴³University of Pittsburgh, Pittsburgh, Pennsylvania 15260, USA
⁴⁴Purdue University, West Lafayette, Indiana 47907, USA
⁴⁵University of Rochester, Rochester, New York 14627, USA
⁴⁶The Rockefeller University, New York, New York 10065, USA
⁴⁷Istituto Nazionale di Fisica Nucleare, Sezione di Roma 1,
^{jj}Sapienza Università di Roma, I-00185 Roma, Italy
⁴⁸Rutgers University, Piscataway, New Jersey 08855, USA
⁴⁹Texas A&M University, College Station, Texas 77843, USA
⁵⁰Istituto Nazionale di Fisica Nucleare Trieste/Udine,
I-34100 Trieste, ^{kk}University of Udine, I-33100 Udine, Italy
⁵¹University of Tsukuba, Tsukuba, Ibaraki 305, Japan
⁵²Tufts University, Medford, Massachusetts 02155, USA
⁵³University of Virginia, Charlottesville, Virginia 22906, USA
⁵⁴Waseda University, Tokyo 169, Japan
⁵⁵Wayne State University, Detroit, Michigan 48201, USA
⁵⁶University of Wisconsin, Madison, Wisconsin 53706, USA
⁵⁷Yale University, New Haven, Connecticut 06520, USA

An inclusive search for the standard model Higgs boson using the four-lepton final state in proton-antiproton collisions produced by the Tevatron at $\sqrt{s} = 1.96$ TeV is conducted. The data are recorded by the CDF II detector and correspond to an integrated luminosity of 9.7 fb^{-1} . Three distinct Higgs decay modes, namely ZZ , WW , and $\tau\tau$, are simultaneously probed. Nine potential signal events are selected and found to be consistent with the background expectation. We set a 95% credibility limit on the production cross section times the branching ratio and subsequent decay to the four lepton final state for hypothetical Higgs boson masses between $120 \text{ GeV}/c^2$ and $300 \text{ GeV}/c^2$.

The vector gauge bosons mediating the weak force, the W and Z , are massive. Within the standard model of

particle physics (SM) their masses arise through spontaneous symmetry breaking (SSB) of the electroweak symmetry [1–3] through the introduction of a scalar field that maintains the gauge invariance of the theory [4–7]. Fundamental fermions may acquire mass through Yukawa couplings with this field. Quantization of the field necessitates the existence of an associated spin-0 particle, known as the Higgs boson, the discovery of which would confirm the SM mechanism for electroweak SSB.

Direct searches at LEP [8], combined with recent search results from the Tevatron [9] and LHC experiments [10, 11], exclude all potential SM Higgs masses outside the ranges $116.6 - 119.4 \text{ GeV}/c^2$ and $122.1 - 127 \text{ GeV}/c^2$. Although signal processes leading to four-lepton final states are not the most dominant within these mass ranges the inclusion of additional channels improves overall search sensitivity. Moreover, using the new techniques presented here, the search is simultaneously sensitive to multiple production and decay modes. Also based on this inclusive approach, information regarding Higgs boson couplings to both fermions and bosons can be extracted, which could be useful to probe the SM or beyond SM nature of a hypothetical signal.

Searches for the SM Higgs boson to four leptons through the decay $ZZ^{(*)}$ have been published by ATLAS [12] and CMS [13] using proton-proton collision data at a center of mass energy of 7 TeV. In this Letter a

*Deceased

†With visitors from ^aIstituto Nazionale di Fisica Nucleare, Sezione di Cagliari, 09042 Monserrato (Cagliari), Italy, ^bUniversity of CA Irvine, Irvine, CA 92697, USA, ^cUniversity of CA Santa Barbara, Santa Barbara, CA 93106, USA, ^dUniversity of CA Santa Cruz, Santa Cruz, CA 95064, USA, ^eInstitute of Physics, Academy of Sciences of the Czech Republic, Czech Republic, ^fCERN, CH-1211 Geneva, Switzerland, ^gCornell University, Ithaca, NY 14853, USA, ^hUniversity of Cyprus, Nicosia CY-1678, Cyprus, ⁱOffice of Science, U.S. Department of Energy, Washington, DC 20585, USA, ^jUniversity College Dublin, Dublin 4, Ireland, ^kETH, 8092 Zurich, Switzerland, ^lUniversity of Fukui, Fukui City, Fukui Prefecture, Japan 910-0017, ^mUniversidad Iberoamericana, Mexico D.F., Mexico, ⁿUniversity of Iowa, Iowa City, IA 52242, USA, ^oKinki University, Higashi-Osaka City, Japan 577-8502, ^pKansas State University, Manhattan, KS 66506, USA, ^qEwha Womans University, Seoul, 120-750, Korea, ^rUniversity of Manchester, Manchester M13 9PL, United Kingdom, ^sQueen Mary, University of London, London, E1 4NS, United Kingdom, ^tUniversity of Melbourne, Victoria 3010, Australia, ^uMuons, Inc., Batavia, IL 60510, USA, ^vNagasaki Institute of Applied Science, Nagasaki, Japan, ^wNational Research Nuclear University, Moscow, Russia, ^xNorthwestern University, Evanston, IL 60208, USA, ^yUniversity of Notre Dame, Notre Dame, IN 46556, USA, ^zUniversidad de Oviedo, E-33007 Oviedo, Spain, ^{aa}CNRS-IN2P3, Paris, F-75205 France, ^{bb}Texas Tech University, Lubbock, TX 79609, USA, ^{cc}Universidad Tecnica Federico Santa Maria, 110v Valparaiso, Chile, ^{dd}Yarmouk University, Irbid 211-63, Jordan,

search for the Higgs boson produced inclusively and decaying into final states containing either four electrons ($4e$), four muons (4μ) or two electrons and two muons ($2e2\mu$) is reported. Data from proton-antiproton collisions at center of mass energy 1.96 TeV, collected with the CDF II detector [14] at the Tevatron and corresponding to 9.7 fb^{-1} of integrated luminosity, are used. Higgs boson decays to Z boson pairs ($H \rightarrow ZZ$) are the dominant contribution for most of the considered Higgs boson mass range. Owing to the full reconstruction of the final state, the ZZ channel provides good search sensitivity in spite of the small potential signal yields because the resonance structure of the signal can be exploited to distinguish it from non-resonant backgrounds. Along with the direct Higgs production mechanisms of gluon-fusion (ggH) and fusion of vector bosons emitted from the incoming partons (VBF), the search is sensitive to associated Higgs boson production processes (VH). In the case of ZH production, additional potential four-lepton event contributions originate from Higgs boson decays to W boson pairs ($ZH \rightarrow ZWW \rightarrow ll\nu\nu$) and τ -lepton pairs ($ZH \rightarrow Z\tau\tau \rightarrow ll\nu\nu$). The detection of four leptons provides one of the cleanest signatures available at a hadron collider. Because of the small probability associated with mimicking the signature of isolated lepton candidates in the detector, background contributions from ubiquitous multi-jet production processes are negligible in this final state.

Separation of potential signal and background event contributions is obtained from the observed four-lepton invariant mass ($m_{4\ell}$) and missing transverse energy spectra [36]. Sensitivity is significantly enhanced through the inclusion of \cancel{E}_T information since $H \rightarrow WW$ and $H \rightarrow \tau\tau$ decays to leptons result in final state neutrinos, while none are expected in background events. The inclusion of \cancel{E}_T significantly improves the search sensitivity at Higgs masses below $150 \text{ GeV}/c^2$, and represents the main advancement in analysis technique over previously published searches in this final state.

Our search is performed using the CDF II detector consisting of a solenoidal spectrometer with a silicon tracker and an open-cell drift chamber (COT) surrounded by calorimeters and muon detectors [14]. The geometry is characterized using the azimuthal angle ϕ and the pseudorapidity η . Transverse energy, E_T , is defined as $E \sin \theta$, where E is the energy of an electromagnetic or hadronic calorimeter energy cluster. Transverse momentum, p_T , is the track momentum component transverse to the beam line.

Electron candidates are identified by matching a central or forward track to energy deposited within the calorimeter. Muon candidates are formed from charged particle tracks matched to minimum ionizing energy deposition in the calorimeter, which may or may not be matched to track segments (*stubs*) in the muon chambers situated behind the calorimeters. Lepton reconstruction

algorithms are well validated and described in detail elsewhere [14]. Taus are included in this search only if they decay to electrons or muons.

Candidate leptons are separated into various categories: electrons, muons, and isolated tracks that project to detector regions with insufficient calorimeter coverage for energy measurements. Electron candidates are distinguished by whether they are found in the central or forward calorimeters ($|\eta| > 1.1$) where only silicon tracking information is available. The electron selection relies on track quality, track-calorimeter matching, calorimeter energy, calorimeter profile shape, and isolation information. Most muon candidates rely on direct detection in the muon chambers, which are distinguished by their acceptance in pseudorapidity: central muon detectors ($|\eta| < 0.6$), central muon extension detectors ($0.6 < |\eta| < 1.0$), and the intermediate muon detector ($1.0 < |\eta| < 1.5$). Remaining muon candidates rely on track matches to energy deposits consistent with a minimum ionizing charged particle in the central and forward electromagnetic calorimeters respectively, failing to have an associated stub in the muon sub-detectors. Isolated tracks pointing to uninstrumented regions of the detector and satisfying high-quality requirements are reconstructed as leptons of unidentified flavor. All leptons are required to be isolated by imposing the condition that the sum of the transverse energy of the calorimeter towers in a cone of $\Delta R \equiv \sqrt{(\Delta\phi)^2 + (\Delta\eta)^2} = 0.4$ around the lepton is less than 10% of the electron E_T (muon p_T). A similar isolation requirement is applied based on the reconstructed tracks in a $\Delta R = 0.4$ cone around the lepton candidate track.

The probability that a jet will be misidentified as a lepton is measured using jet-enriched samples and is corrected for the contributions of leptons from W and Z boson decays. An average value is obtained from samples collected with different single jet E_T threshold requirements (20, 50, 70, and 100 GeV) and an uncertainty is assigned based on the spread within the individual measurements. The range of measured misidentification probabilities for the lepton categories, which vary according to E_T or p_T , is 0.5% – 3% (central electrons), 2% – 6% (forward electrons), 0.5% – 4% (central muons), 0.5% – 2% (extension muons), 0.5% – 2% (intermediate muons), 0.5% – 6% (calorimeter only muons), and 0.5% – 3% (isolated tracks).

Events for the analysis are collected using online event selection (trigger) requirements corresponding to the presence of a single high- E_T electron or high- p_T muon. The electron trigger requires an electromagnetic energy cluster in the central calorimeter with $E_T > 18 \text{ GeV}$ geometrically matching the direction of a charged particle reconstructed in the COT with $p_T > 8 \text{ GeV}/c$. Muon triggers are based on track segments in the muon chambers geometrically matching the direction of a charged particle reconstructed in the COT with $p_T > 18 \text{ GeV}/c$.

Trigger efficiencies are measured using samples of leptonic Z decays [14]. To ensure a uniform trigger efficiency over the lepton momentum spectra, an offline selection is applied to the lepton matched to the trigger object, requiring $E_T > 20$ GeV ($p_T > 20$ GeV/ c) for electrons (muons).

Additional charged electrons (muons) are required to have $E_T > 10$ GeV ($p_T > 10$ GeV/ c). Exactly four leptons are required, each separated from the others by $\Delta R \geq 0.1$. This analysis evolved from a CDF measurement of the ZZ production cross section in the four lepton final state [15], where constraints on the invariant mass of opposite-sign same-flavor dilepton pairs were imposed in order to explicitly reconstruct Z bosons. For Higgs boson masses smaller than 180 GeV/ c^2 , at least one of the Z bosons is off-shell and such requirements on the mass become inefficient. We therefore require dilepton pair masses to be between 20 and 140 GeV/ c^2 . In the final state where all leptons are of the same flavor, opposite-sign pairings are assigned based on the the smallest deviation of the reconstructed masses from the known Z boson mass. Because the backgrounds are modest, loose constraints on the mass improve the sensitivity of the search. Higgs boson production can also involve hadronic jets originating from the associated vector boson in WH or ZH production, the additional quarks in the forward detector from VBF production, or initial state gluon radiation. Therefore, we place no restriction on the number of reconstructed jets contained within each event.

The selected events consist primarily of the background from non-resonant diboson production of Z^*/Z -boson pairs (ZZ). Smaller contributions originate from non-fully leptonic ZZ decays and $Z\gamma$ production, which lead to events with two or three real reconstructed leptons and one or two falsely reconstructed leptons associated with the photon or additional hadronic jet activity. The background from top-quark pair production is found to be negligible (<0.01 events).

The acceptances, efficiencies and kinematic properties of the signal and background processes are determined from simulation. PYTHIA [16] is used to model all Higgs boson production processes and the non-resonant ZZ background. The modeling of $Z\gamma$ is based on the simulation framework developed by Bauer and Berger [17]. For all samples CTEQ5L parton distribution functions (PDFs) are used to model the momentum distribution of the initial-state partons [18]. The cross sections for each process are normalized to next-to-next-to-leading order (NNLO) calculations with logarithmic resummation for ggH [19, 20], NNLO for VH [21–23], and next-to-leading order (NLO) calculations for VBF [21, 24], ZZ [25], and $Z\gamma$ [26].

The response of the CDF II detector is modeled with a GEANT-based simulation [27]. Efficiency corrections for the simulated CDF II detector response for leptons and photon conversions were determined using independent

data samples.

The overall normalization of the estimated background from false leptons is derived using a data-driven approach while the shape of the distribution is derived from MC simulation. The total contribution from false lepton events is estimated using events with two or three leptons and additional jets that may be falsely reconstructed as leptons weighted by the measured jet-to-lepton misidentification probabilities. Since the number of available three-lepton events in data is small, we model kinematic distributions using a weighted sum of those obtained from the simulated ZZ and $Z\gamma$ MC samples.

The kinematic distributions of ZZ events with falsely reconstructed leptons is assumed to be the same as that for correctly reconstructed ZZ events. We apply the same procedure to the simulated $Z\gamma$ sample to obtain the invariant mass distribution for events from this process, which are found to be well modeled by a Landau function. We model \cancel{E}_T in $Z\gamma$ events using the distribution from simulated ZZ events with falsely reconstructed leptons, which was found to agree.

In the ranges $50 < m_{4l} < 600$ GeV/ c^2 and $0 < \cancel{E}_T < 200$ GeV, we estimate background contributions of 10.59 ± 1.34 ZZ events and 0.39 ± 0.19 events with falsely reconstructed leptons. For a SM Higgs boson with a mass of 125 GeV/ c^2 , contributions of 0.053 (ggH), 0.003 (VBF), 0.006 (WH), and 0.089 (ZH) events, yielding a total of 0.15 ± 0.01 events, are expected. The indicated uncertainties include statistical and systematic contributions added in quadrature. Systematic uncertainties are described below.

We observe a total of nine events, which is consistent with the rate expected from background sources only. The four-lepton invariant mass and \cancel{E}_T distributions are shown in Fig. 1(a) and Fig. 1(b) respectively, both overlaid with expected contributions from backgrounds and Higgs boson production for a mass of 125 GeV/ c^2 , shown separately for each production process.

A variety of possible systematic effects were considered including those that affect the normalization and the shape of the kinematic distributions. The dominant systematic uncertainties are those on the theory predictions for the cross sections of signal and background processes. Systematic uncertainties associated with the MC affect Higgs signal, ZZ , and $Z\gamma$ acceptances determined from the simulated event samples.

Uncertainties originating from lepton selection and trigger efficiency measurements are propagated through the acceptance calculation, leading to uncertainties of 3.6% and 0.5% , on the predicted signal and background event yields, respectively. In addition, all signal and background estimates obtained from simulation have an additional 5.9% uncertainty originating from the measurement of the luminosity [28].

The $gg \rightarrow H$ cross-section has been computed at NNLO and next-to-next-to-leading log (NNLL) preci-

sion varying the renormalization and factorization scales and implementing different correlated combinations of the MSTW2008 error PDFs together with allowed values of the strong coupling constant (α_s) [29, 30], yielding systematic uncertainties of 7.0% and 7.7%, respectively. Uncertainties on VBF and associated Higgs boson production, which account for about a quarter of the total Higgs boson events in our sample, are of 5% and 10%, respectively [31]. A 3% uncertainty was assigned on the branching fraction for $H \rightarrow ZZ$ and $H \rightarrow WW$, which are 100% correlated, as well as a 3% uncorrelated uncertainty on $H \rightarrow \tau\tau$ [31]. The PYTHIA MC simulation for ZZ production that is used for determining acceptances is based on an expansion at LO; MCFM [32] was used to estimate the potential difference in the acceptance arising from a full NLO simulation, estimated to be $\pm 2.5\%$ and assigned as a systematic uncertainty. We assign a 10% uncertainty on the ZZ cross-section based on the difference between LO and NLO [33] predictions. The $Z\gamma$ component was parametrized using a Landau distribution, where an uncorrelated 50% uncertainty was assigned to the yield prediction in each bin to fully cover the possible effects of mis-modeling. Misidentification probabilities were measured in several jet samples and the maximum spread between these measurements was assigned as a systematic uncertainty on the background estimation. Propagated through to the acceptance, this technique results in a 50% variation in the estimate of the background from fake leptons. The missing transverse energy is scaled up and down by 20% to account for potential MC mis-modeling, and the modified shapes are taken as shape uncertainties on the MC \cancel{E}_T distributions used as inputs to the limit calculation.

Only three \cancel{E}_T bins (0–15, 15–45, and 45–200 GeV) are used in the limit setting procedure. The varied spacing was chosen as a compromise between search sensitivity and ensuring sufficient number of simulated events in each bin.

As a cross-check the distribution of the number of jets per event in data was compared to the expectation from the ZZ MC simulation and found to be consistent.

Upper limits at the 95% credibility level (C.L.) are set on the Higgs boson production cross section, σ_H , as a function of m_H . A Bayesian technique [34] was employed, where the posterior probability density was constructed from the joint Poisson probability of observing the data in each bin of the $m_{4l}-\cancel{E}_T$ space, integrating over the uncertainties of the normalization parameters using Gaussian priors. A non-negative constant prior in the signal rate was assumed. The expected limit and associated one and two sigma bands are shown along with the observed limit in Table I and Fig. 2. For a Higgs boson with $m_H = 125 \text{ GeV}/c^2$ we expect a sensitivity of $26.5 \times \sigma_{SM}$ at 95% C.L. while we observe a limit of $29.3 \times \sigma_{SM}$ at 95% C.L. . The results obtained in the investigated mass range are consistent with the observed event excess near

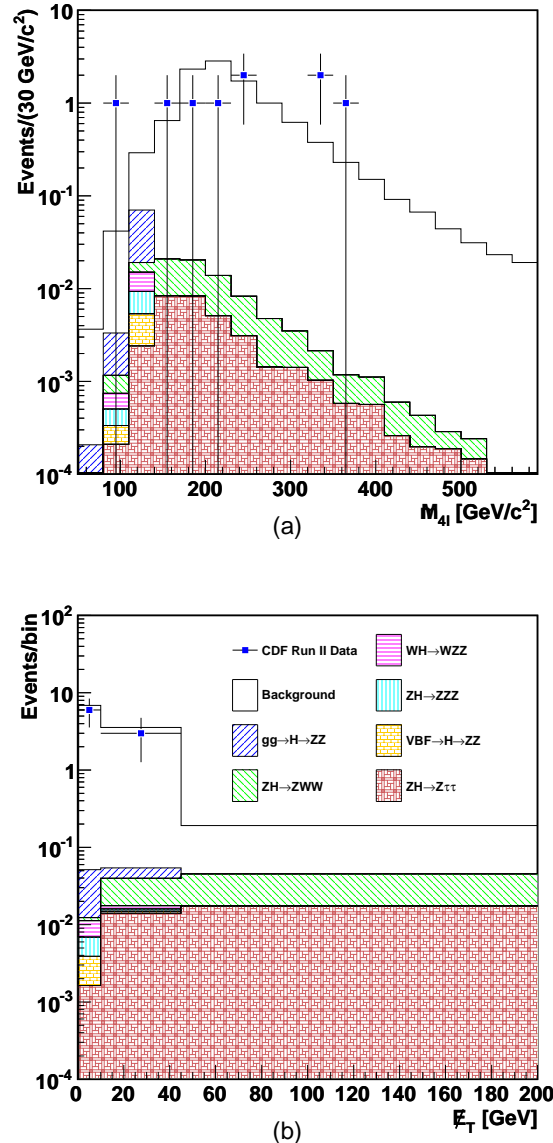


FIG. 1: Distributions of the four-lepton invariant mass (a) and the missing transverse energy (b) in data. The combined estimated contribution from non-resonant ZZ production and fake leptons, denoted as background, is overlaid. The potential contributions of the different Higgs production processes for $m_H = 125 \text{ GeV}/c^2$ are stacked and also overlaid.

$325 \text{ GeV}/c^2$ in the CDF search for high-mass resonances decaying to ZZ [35]. The analysis reported here is performed using standard CDF tracking algorithms while [35] uses an alternative reconstruction.

In 9.7 fb^{-1} of integrated luminosity collected at the Tevatron, no evidence for a Higgs boson signal is found in the mass range explored. Upper limits on the Higgs boson production cross section in the inclusive four-lepton final state relative to the SM expectation are obtained. Maximal search sensitivity is obtained not only in the

TABLE I: Expected and observed upper limits on the Higgs boson production relative to the SM prediction for Higgs particle masses from 120 GeV/c² to 300 GeV/c².

H → 4ℓ	120	130	140	150	160	170	180	190	200	210	220	230	240	250	260	270	280	290	300
Expected/σ _{SM}	38.0	18.3	11.7	9.4	16.0	25.1	18.5	9.8	10.6	12.9	15.7	16.6	18.9	20.5	21.1	23.2	23.5	28.0	30.5
Observed/σ _{SM}	42.4	20.5	12.6	9.5	16.8	28.5	16.3	8.2	7.2	7.9	10.3	20.5	21.1	17.4	17.3	18.2	19.9	24.1	28.6

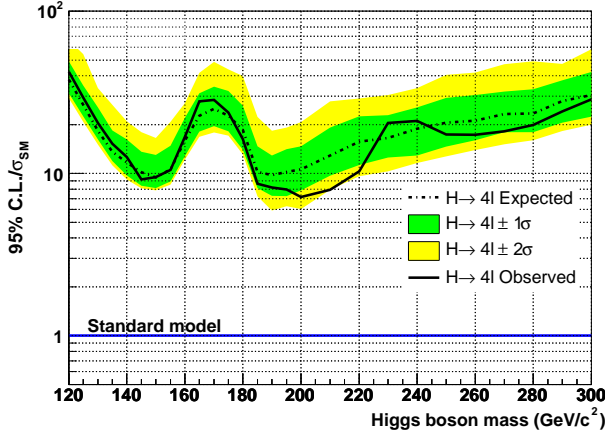


FIG. 2: Expected and observed upper limits on the Higgs boson production relative to the SM prediction as a function of Higgs boson mass.

high mass region where both Z bosons are produced on-shell but also in the lower mass region around 150 GeV/c² where additional signal contributions from $ZH \rightarrow ZWW$ and $ZH \rightarrow Z\tau\tau$ improve the sensitivity by 15%.

We thank the Fermilab staff and the technical staffs of the participating institutions for their vital contributions. This work was supported by the U.S. Department of Energy and National Science Foundation; the Italian Istituto Nazionale di Fisica Nucleare; the Ministry of Education, Culture, Sports, Science and Technology of Japan; the Natural Sciences and Engineering Research Council of Canada; the National Science Council of the Republic of China; the Swiss National Science Foundation; the A.P. Sloan Foundation; the Bundesministerium für Bildung und Forschung, Germany; the Korean World Class University Program, the National Research Foundation of Korea; the Science and Technology Facilities Council and the Royal Society, UK; the Russian Foundation for Basic Research; the Ministerio de Ciencia e Innovación, and Programa Consolider-Ingenio 2010, Spain; the Slovak R&D Agency; the Academy of Finland; and the Australian Research Council (ARC).

[1] S. Glashow, Nucl.Phys. **22**, 579 (1961).

[2] A. Salam, in *Elementary Particle Theory*, p. 367

(Almquist and Wiksell, Stockholm, 1968).

[3] S. Weinberg, Phys. Rev. Lett. **19**, 1264 (1967).

[4] P. W. Higgs, Phys. Lett. **12**, 132 (1964).

[5] P. W. Higgs, Phys. Rev. Lett. **13**, 508 (1964).

[6] G. Guralnik, C. Hagen, and T. Kibble, Phys. Rev. Lett. **13**, 585 (1964).

[7] F. Englert and R. Brout, Phys. Rev. Lett. **13**, 321 (1964).

[8] The ALEPH, DELPHI, L3 and OPAL Collaborations, and the LEP Working Group for Higgs boson searches, Phys. Lett. B **565**, 61 (2003).

[9] The CDF and D0 Collaborations and the Tevatron New Physics and Higgs Working Group (2012), arXiv:1207.0449v2.

[10] G. Aad *et al.* (ATLAS Collaboration) (2012), arXiv:1207.0319v1.

[11] S. Chatrchyan *et al.* (CMS Collaboration), Phys. Lett. B **710**, 26 (2012), arXiv:1202.1488.

[12] G. Aad *et al.* (Atlas Collaboration), Phys. Lett. B **710**, 383 (2012).

[13] S. Chatrchyan *et al.* (CMS Collaboration) (2012), 1202.1997.

[14] A. Abulencia *et al.* (CDF Collaboration), J. Phys. G **34**, 2457 (2007).

[15] T. Aaltonen *et al.* (CDF Collaboration), Phys. Rev. Lett. **108**, 101801 (2012).

[16] T. Sjostrand, S. Mrenna, and P. Skands, J. High Energy Phys. **05**, 026 (2006).

[17] U. Baur and E. L. Berger, Phys. Rev. D **47**, 4889 (1993).

[18] H. L. Lai *et al.* (CTEQ), Eur. Phys. J. C **12**, 375 (2000).

[19] D. de Florian and M. Grazzini, Phys. Lett. B **674**, 291 (2009).

[20] C. Anastasiou, R. Boughezal, and F. Petriello, J. High Energy Phys. **04**, 003 (2009).

[21] K. Assamagan *et al.* (Higgs Working Group Collaboration), pp. 1–169 (2004), hep-ph/0406152.

[22] O. Brein, A. Djouadi, and R. Harlander, Phys. Lett. B **579**, 149 (2004).

[23] M. L. Ciccolini, S. Dittmaier, and M. Kramer, Phys. Rev. D **68**, 073003 (2003).

[24] E. L. Berger and J. M. Campbell, Phys. Rev. D **70**, 073011 (2004).

[25] J. Campbell and R. K. Ellis, *MCFM - Monte Carlo for FeMtobarn processes* (2010), We ran MCFM Monte Carlo with the MSTW2008 PDF set and varying the factorization and renormalization scale.

[26] U. Baur, T. Han, and J. Ohnemus, Phys. Rev. D **57**, 2823 (1998).

[27] R. Brun, R. Hagelberg, M. Hansroul, and J. Lassalle, CERN-DD-78-2-REV and CERN-DD-78-2.

[28] D. Acosta *et al.*, Nucl. Instrum. Meth. A **494**, 57 (2002).

[29] S. Catani and M. Grazzini, Phys. Rev. Lett. **98**, 222002 (2007).

[30] M. Grazzini, J. High Energy Phys. **0802**, 043 (2008).

[31] TeV4LHC, *Standard model higgs*

- cross sections at hadron colliders*, <http://maltoni.home.cern.ch/maltoni/TeV4LHC/SM.html>.
- [32] J. Campbell, K. Ellis, and C. Williams, *Monte carlo for femtobarn processes*, <http://mcfm.fnal.gov/mcfm.pdf>.
- [33] J. M. Campbell and R. K. Ellis, Phys. Rev. D **60**, 113006 (1999).
- [34] J. Beringer *et al.* (Particle Data Group), Phys. Rev. D **86**, 010001 (2012).
- [35] T. Aaltonen *et al.* (CDF), Phys. Rev. D **83**, 112008 (2011), 1102.4566.
- [36] The \cancel{E}_T is the magnitude of the missing transverse energy vector $\vec{\cancel{E}}_T$, which is defined as the opposite of the vector sum of the E_T of all calorimetric towers, corrected to produce the correct average calorimeter response to jets and to muons.